

Molecular basis for sterol transport by StART-like lipid transfer domains

Florian A Horenkamp^{1,†} , Diana P Valverde^{1,†}, Jodi Nunnari² & Karin M Reinisch^{1,*} 

Abstract

Lipid transport proteins at membrane contact sites, where two organelles are closely apposed, play key roles in trafficking lipids between cellular compartments while distinct membrane compositions for each organelle are maintained. Understanding the mechanisms underlying non-vesicular lipid trafficking requires characterization of the lipid transporters residing at contact sites. Here, we show that the mammalian proteins in the lipid transfer proteins anchored at a membrane contact site (LAM) family, called GRAMD1a-c, transfer sterols with similar efficiency as the yeast orthologues, which have known roles in sterol transport. Moreover, we have determined the structure of a lipid transfer domain of the yeast LAM protein Ysp2p, both in its apo-bound and sterol-bound forms, at 2.0 Å resolution. It folds into a truncated version of the steroidogenic acute regulatory protein-related lipid transfer (StART) domain, resembling a lidded cup in overall shape. Ergosterol binds within the cup, with its 3-hydroxy group interacting with protein indirectly via a water network at the cup bottom. This ligand binding mode likely is conserved for the other LAM proteins and for StART domains transferring sterols.

Keywords cholesterol; endoplasmic reticulum; lipid transport protein; membrane contact sites; StART domain

Subject Categories Membrane & Intracellular Transport; Structural Biology

DOI 10.15252/emboj.201798002 | Received 14 August 2017 | Revised 2 February 2018 | Accepted 5 February 2018 | Published online 21 February 2018

The EMBO Journal (2018) 37: e98002

Introduction

Lipids, which are synthesized primarily in the endoplasmic reticulum (ER), become redistributed to other compartments asymmetrically. As a result, organelles differ in the composition of their lipid bilayers, imparting different biochemical and biophysical characteristics and helping to define organelle identity (Bigay & Antonny, 2012). Membrane contact sites, where two organelles are closely apposed, and the lipid transfer proteins enriched at such sites play critical roles in lipid redistribution (Lahiri *et al*, 2015; Drin *et al*, 2016; Kentala *et al*, 2016; Reinisch & De Camilli, 2016; Saheki *et al*,

2016). By definition, lipid transport proteins include lipid binding modules which function by solubilizing lipids during transit across the cytosol between two organelle membranes. Some transport proteins additionally serve as tethers, helping to maintain the architecture of contact sites. Identification and characterization of lipid transporters at membrane contact sites are an area of ongoing research critical in unraveling the mechanisms that underlie lipid homeostasis (Schauder *et al*, 2014; Lahiri *et al*, 2015; Drin *et al*, 2016; Kentala *et al*, 2016; Reinisch & De Camilli, 2016; Saheki *et al*, 2016; Lees *et al*, 2017).

The lipid transfer proteins anchored at a membrane contact site (LAM) or lipid transfer at contact site (Ltc) family of lipid transporters was discovered on the basis of distant sequence homology and structural alignment with proteins containing a steroidogenic acute regulatory protein-related lipid transfer (StART) domain (Gatta *et al*, 2015; Murley *et al*, 2015). A number of StART proteins transfer sterol, whereas others are involved in the transport of other lipids such as ceramide, phosphatidylcholine, or bile acids (Clark, 2012; Alpy & Tomasetto, 2014; Letourneau *et al*, 2015). Proteins in the LAM/Ltc family all feature an unstructured N-terminus, followed by a pleckstrin homology-like domain known as a GRAM domain, one or two StART-like domains, a transmembrane segment anchored to the ER, and a short ER-luminal stretch (Gatta *et al*, 2015; Murley *et al*, 2015; Fig 1A). Although there are no known StART domain proteins in *S. cerevisiae*, there are six LAM/Ltc proteins with StART-like domains, which localize to contacts between the ER and the plasma membrane (PM; Ysp2p/Lam2p/Ltc4p, Lam4p/Ltc3p, Ysp1p/Lam1p, Sip3p/Lam3p; Gatta *et al*, 2015) or either ER-mitochondrial or ER-vacuolar contacts (Lam5p/Ltc2p, Lam6p/Ltc1p) (Elbaz-Alon *et al*, 2015; Murley *et al*, 2015). Characterized yeast LAM/Ltc proteins all bind and/or transport sterol (Gatta *et al*, 2015; Murley *et al*, 2015) and have been implicated in coordinating sterol homeostasis with cellular stress responses (Murley *et al*, 2017). We show here that the three mammalian LAM/Ltc proteins, called GramD1a-c, all efficiently transport sterols *in vitro* and so are also likely to function in sterol transport, perhaps with similar roles in stress response as in fungi. How the LAM/Ltc proteins, or related proteins in the StART family, interact with sterol has so far been unknown.

To address how StART and StART-like proteins bind sterol, we determined the crystal structure of a StART-like domain of

1 Department of Cell Biology, Yale University School of Medicine, New Haven, CT, USA

2 Department of Molecular and Cellular Biology, University of California, Davis, Davis, CA, USA

*Corresponding author. Tel: +1 203 785 6469; E-mail: karin.reinisch@yale.edu

†These authors contributed equally to this work

S. cerevisiae Ysp2p both in its apo- and ergosterol-bound forms at 2.0 Å resolution. The StART-like domain is a truncated variation of the α/β helix-grip fold found in StART modules (Tsujishita & Hurley, 2000; Romanowski *et al.*, 2002; Thorsell *et al.*, 2011), forming a cup-like structure with a lid. Ergosterol binds within the cup, inducing a conformational change that results in lid closure and shields bound lipid from the aqueous environment. The ergosterol moiety occupies only the upper two thirds of the cavity, whose sides are lined with hydrophobic residues. Its 3-hydroxyl group interacts with protein indirectly via a network of water molecules in the bottom third of the cavity, which are hydrogen bonded to hydrophilic residues located there. This mode of sterol binding likely is conserved in other LAM/Ltc as well as in sterol binding StART proteins.

Results and Discussion

The StART-like domains of the human LAM/Ltc proteins and Ysp2p transfer sterols between membranes *in vitro*

To determine whether the StART-like domains of the mammalian LAM/Ltc proteins transport sterols, we expressed and purified constructs containing the StART-like domain of human GramD1a (residues 363–565), GramD1b (residues 372–572), and GramD1c (residues 323–521) (Fig 1A) and assayed their transfer ability *in vitro*. For comparison, we also tested the Osh4p protein, one of the best studied sterol transporters (Im *et al.*, 2005; Raychaudhuri *et al.*, 2006; de Saint-Jean *et al.*, 2011; Moser von Filseck *et al.*, 2015b), as well as the StART-like domains of Ysp2p, whose ability to extract and bind sterols was reported previously (Gatta *et al.*, 2015), either individually or together (Ysp2p_{S1}: residues 851–1,017; Ysp2p_{S2}: residues 1,027–1,244; Ysp2p_{S1S2}: residues 851–1,244). Except for Ysp2p_{S1}, the constructs also included a conserved, predicted disordered polybasic segment C-terminal to the StART-like module, not present downstream of Ysp2p_{S1}, which increased expression levels and solubility. We used an established fluorescence resonance energy transfer (FRET) assay (Moser von Filseck *et al.*, 2015b) to monitor the transfer of dehydroergosterol (DHE), a fluorescent analog of ergosterol, from a population of donor (L_D) to acceptor (L_A) liposomes (Fig 1B). The liposome preparations were similar, consisting primarily of egg phosphatidylcholine (egg PC), except that the donor liposomes additionally contained DHE (5 mol%) and 1,2-dioleoyl-sn-glycero-3-phosphoethanolamine-N-(5-dimethylamino-1-naphthalenesulfonyl) (DNS-PE, 2.5 mol%). In this assay, the amount of DHE transfer is proportional to the loss of FRET between DHE and DNS-PE in the donor liposomes. All StART domains tested transferred DHE between liposomes (Figs 1C–E and EV1), with transfer rates between ~0.5 and 1.5 DHE/min/molecule, except for GramD1a which transferred ~8.4 molecules DHE/min (Figs 1C and E, and EV1A). The StART-like modules of Ysp2p, likely the result of domain duplication, appear to function independently since the transfer rates of Ysp2p_{S1} and Ysp2p_{S1S2} are similar. Removing the polybasic C-terminal segment from GramD1b (GramD1b_{Short}, residues 372–550) did not negatively affect DHE transport rates (Figs 1C and E, and EV1A). For Osh4p, we calculated a “transfer” rate of ~0.65 molecules DHE/min (Figs 1D and E, and EV1B), similar to values reported previously under slightly different assay conditions (Moser von Filseck *et al.*, 2015b) and similar to

rates for the Ysp2p constructs, GramD1b and GramD1c. (Note, though, that Osh4p transfers plateaus at a value equivalent to the molar quantity of Osh4p (Fig 1D; see also Fig 2A in Moser von Filseck *et al.*, 2015b), suggesting that the decrease in FRET observed for Osh4p is due not to transfer per se but rather to a fast extraction step which is followed by inefficient delivery.)

Membrane composition, which affects the ease with which lipids can be extracted from and inserted into donor or acceptor membranes, respectively, is well known to affect lipid transport rates (Wong *et al.*, 2017), and *in vivo* rates often are much faster than those measured *in vitro* using non-physiological membrane compositions (Wong *et al.*, 2017). To assess the effect of membrane composition on transfer rates, we repeated the transfer assays for two of the protein constructs, Ysp2p_{S1} and GramD1b, while altering donor or acceptor liposome compositions. Since Ysp2p functions at ER–plasma membrane contact sites whereas other LAM/Ltc proteins may function at contacts between the ER and internal organelles like mitochondria or vacuoles (Elbaz-Alon *et al.*, 2015; Gatta *et al.*, 2015; Murley *et al.*, 2015), we first examined the effect of replacing egg PC, which resembles PC at the PM in its more saturated acyl chain composition, with 1,2-dioleoyl-sn-glycero-3-phosphocholine (DOPC), which more resembles PC in internal compartments, in either the donor or acceptor liposomes or both. For both Ysp2p_{S1} and GramD1b, we found that sterol transfer rates increased by factors of ~2–3 fold when the donor or both donor and acceptor liposome populations contained DOPC instead of egg PC (Figs 2A and EV2A and B). Since anionic lipids in either the donor and/or acceptor membranes have been reported to accelerate transport by other lipid transfer proteins (Mesmin *et al.*, 2011; Iaea *et al.*, 2015; Moser von Filseck *et al.*, 2015b), we next examined the effect of anionic lipids on transfer, finding a twofold to fivefold increase in sterol transfer rates by both Ysp2p_{S1} and GramD1b when 5 mol% brain phosphatidylserine (PS), brain phosphatidylinositol-4-phosphate (PI(4)P), or brain phosphatidylinositol-4,5-bisphosphate (PI(4,5)P₂) (Figs 2B and EV2C and D) was added to the acceptor liposomes. Next, we used PM-like and ER-like membrane compositions for the donor (L_{PM}) and acceptor (L_{ER}) liposomes, finding ~20-fold and ~13-fold increases in the Ysp2p_{S1} and GramD1b transfer rates, respectively (Figs 2C and D, and EV2E). In these experiments, the donor liposomes comprised 65% egg PC, 17.5% PE, 10% PS, 5% DHE, and 2.5% DNS-PE, and the acceptor liposomes comprised 78% DOPC, 20% PE, and 2% 1,2-dioleoyl-sn-glycero-3-[(N-(5-amino-1-carboxypentyl) iminodiacetic acid) succinyl] (nickel salt) [DGS-NTA(Ni)]. Finally, since the LAM proteins are thought to localize to contact sites, where the donor and acceptor membranes are in close proximity, we examined the importance of such localization on rate by comparing transport by soluble and tethered protein constructs. The tethered constructs, which include the StART-like domain and surrounding sequences predicted to be unstructured (residues 760–1,058 for Ysp2p-t and residues 208–622 for GramD1b-t), are fused at their N-terminus to the Lactadherin C2 domain, a PS sensor (Yeung *et al.*, 2008) which allows binding to the PS-containing donor liposomes. At their C-terminus, they have a hexahistidine tag, allowing them to interact with DGS-NTA(Ni) in the acceptor liposomes (Fig 2C). Tethering further increases the transfer rate between donor and acceptor liposomes, by a factor of ~2× (Figs 2D and EV2E). This corresponds to a rate enhancement of

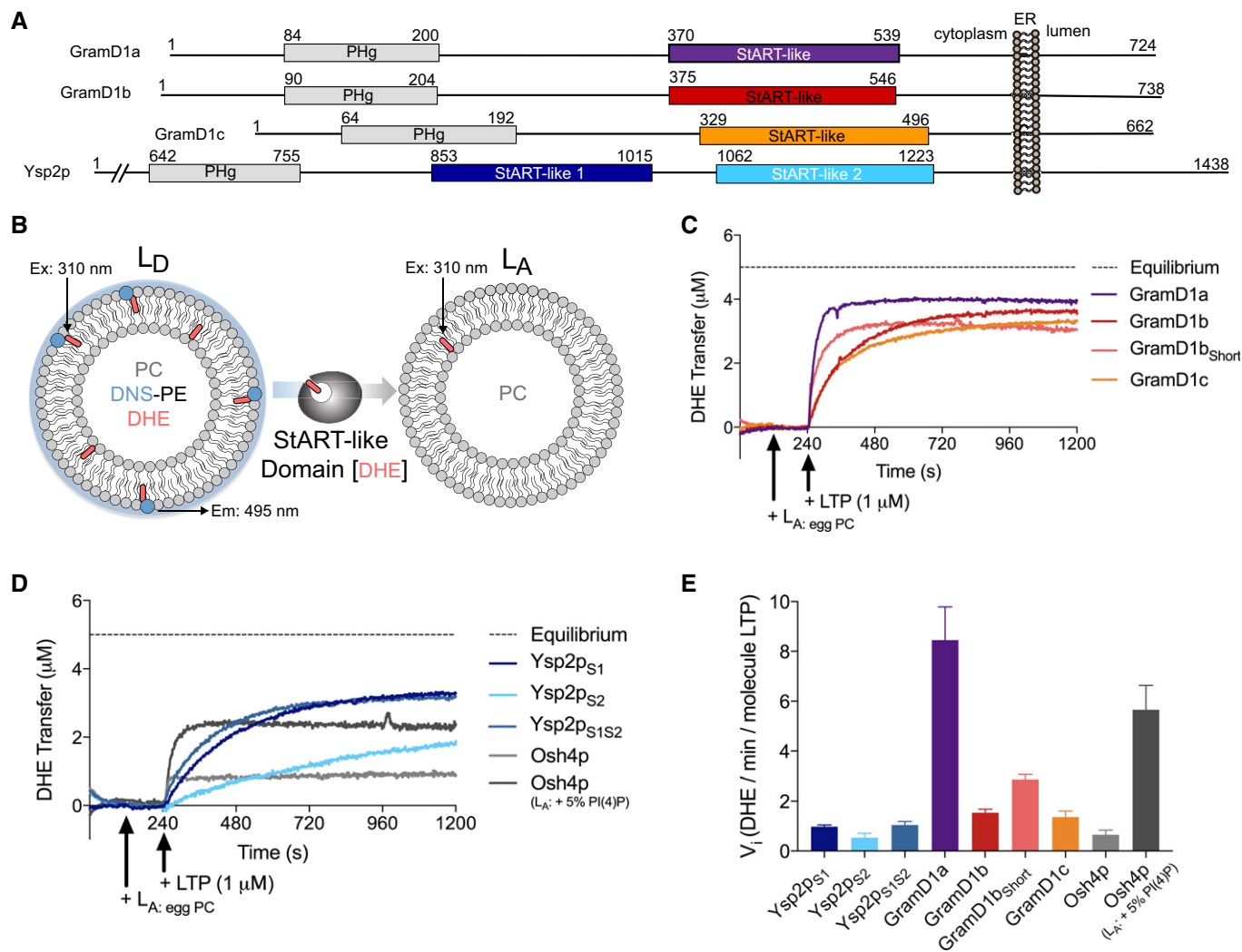


Figure 1. StART-like domains of Ysp2p and GramD1a-c transfer DHE between membranes.

A Domain architecture of Ysp2p and GramD1a-c.
B Schematic of the DHE transport assay. Donor liposomes L_D (92.5/5/2.5 mol% egg PC/DHE/DNS-PE, 200 μM total lipid) were incubated with acceptor liposomes L_A (egg PC, 200 μM total lipid). Transfer of DHE by lipid transfer proteins between L_D and L_A liposomes results in the loss of FRET between DHE and DNS-PE. For reference, the signal of a sample with DHE in equilibrium between L_D (95/2.5/2.5 mol% egg PC/DHE/DNS-PE, 200 μM total lipid) and L_A (97.5/2.5 mol% egg PC/DHE, 200 μM total lipid) was measured. After subtraction of the buffer reaction, the signal was normalized to the amount of DHE present in L_A based on the signal of the equilibrium sample.
C DHE transfer by 1 μM of the StART-like domain of GramD1a (residues 363–565, purple), GramD1b (residues 372–572, red), GramD1b_{Short} (residues 372–550, salmon), and GramD1c (residues 323–521, orange). Mean of three independent experiments. For mean ± SD, see Fig EV1A. The dashed black line represents DHE equilibrium between L_D and L_A.
D DHE transfer by 1 μM of the first (residues 851–1,017, blue), second (residues 1,027–1,244, light blue), or a construct comprising both (residues 851–1,244, steel blue) StART-like domains of Ysp2p or Osh4p (light gray). Addition of 5 mol% PI(4)P to the acceptor liposomes increases Osh4p sterol transfer activity (Osh4p L_A: 5% PI(4)P, dark gray). Mean of three independent experiments. For mean ± SD, see Fig EV1B. The dashed black line represents DHE equilibrium between L_D and L_A.
E Initial DHE transfer rates (V_i, mean ± SD, n = 3).

25–40× (~40 DHE/min/molecule LTP) over those initially measured for sterol transfer by Ysp2p_{S1} and GramD1b with liposomes composed of egg PC (Fig 1E).

To assess whether the StART-like domains preferentially transport sterol, we examined their ability to transfer other lipids, namely phosphatidylethanolamine (PE) and PS. We monitored the transfer of radiolabeled PE (14C) (and cholesterol (3H) as a positive control) between “heavy” and “light” liposomes, containing 0.75 M or no

sucrose, respectively, by scintillation counting after separating the liposomes by centrifugation. We used another established FRET-based assay to follow PS transfer (Moser von Filseck *et al*, 2015a; Fig 3A). The transfer reaction was carried out in the presence of NBD-labeled PS sensor (NBD-C2_{Lact}), with donor liposomes containing 5 mol% brain PS and 2 mol% 1,2-dioleoyl-*sn*-glycero-3-phosphoethanolamine-N-(lissamine rhodamine B sulfonyl) (Rhod-PE). The fluorescence of NBD-C2_{Lact} is quenched by Rhod-PE in the

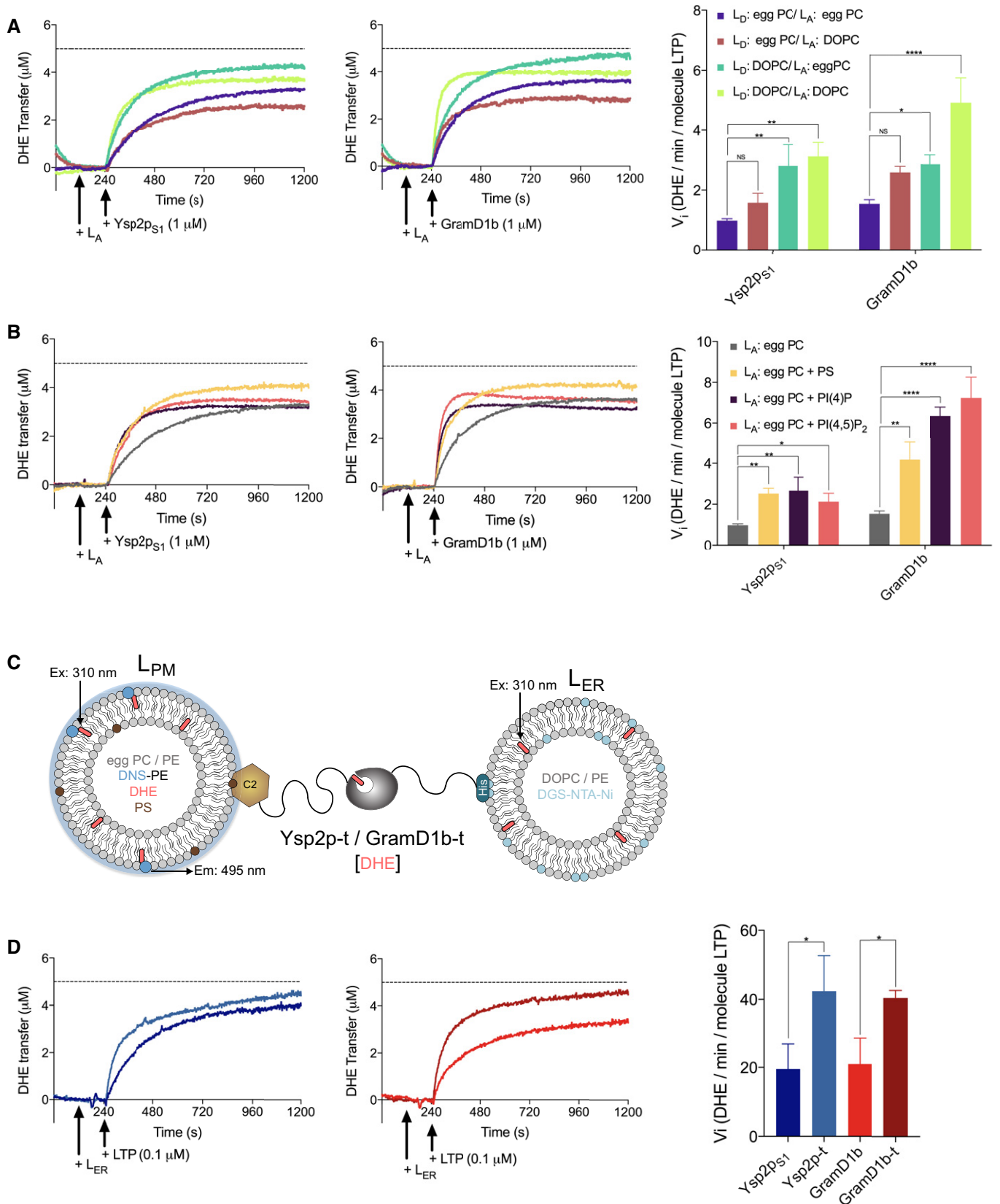


Figure 2.

Figure 2. Membrane composition affects DHE transfer rates of the GramD1b StART-like domain and Ysp2_{S1}.

- A DHE transfer by 1 μM Ysp2p_{S1} or the StART-like domain of GramD1b between liposomes with different acyl chain compositions. Donor liposomes contained 5 mol% DHE, 2.5 mol% DNS-PE, and either 92.5 mol% egg PC (L_D; egg PC) or DOPC (L_D; DOPC). Acceptor liposomes contained either egg PC (L_A; egg PC) or DOPC (L_A; DOPC). The results of the L_D: egg PC to L_A: egg PC transfer are included in Fig 1D and are repeated here for reference. For mean \pm SD, see Fig EV2A and B. The dashed black line represents DHE equilibrium between L_D and L_A. Initial DHE transfer (V_i, mean \pm SD, n = 3. *P < 0.05, **P < 0.01, ****P < 0.0001, NS: not significant). ANOVA with Dunnett's multiple comparisons test.
- B DHE transport by 1 μM Ysp2p_{S1} or the StART-like domain of GramD1b using acceptor liposomes L_A containing egg PC only (gray) or additionally containing 5 mol% of either PS (yellow), PI(4)P (purple), or PI(4,5)P₂ (red). The results of the L_D: egg PC to L_A: egg PC transfer are included in Fig 1 and are repeated here for reference. Mean of three independent experiments. For mean \pm SD, see Fig EV2C and D. The dashed black line represents DHE equilibrium between L_D and L_A. Initial DHE transfer rates (V_i, mean \pm SD, n = 3. *P < 0.05, **P < 0.01, ****P < 0.0001, NS: not significant). ANOVA with Dunnett's multiple comparisons test.
- C To tether Ysp2p_{S1} and the StART-like domain of GramD1b to liposomes, we added surrounding sequences predicted to be unstructured (residues 760–1,058 for Ysp2p and residues 208–622 for GramD1b) and fused them with the Lactadherin C2 domain at their N-terminus, allowing for binding to PS-containing donor liposomes (L_{PM}), and a hexahistidine tag at their C-terminus, allowing interaction with DGS-NTA(Ni) in the acceptor liposomes (L_{ER}).
- D DHE transport from PM-like (L_{PM}) to ER-like (L_{ER}) liposome populations by Ysp2p_{S1} (blue) and the StART-like domain of GramD1b (red) or by membrane-tethered Ysp2p-t (light blue) and GramD1b-t (brown) (0.1 μM final protein concentration). Mean of three independent experiments. For mean \pm SD, see Fig EV2E. The dashed black line represents DHE equilibrium between L_{PM} and L_{ER}. Initial DHE transfer rates (V_i, mean \pm SD, n = 3). *P < 0.05. Unpaired, two-tailed t-test.

donor liposomes, and an increase in NBD fluorescence is observed if PS and consequently the probe are removed from the donor liposomes and transferred to the acceptor liposomes. We did not observe transfer of PE (Fig 3B) or PS (Figs 3C and D, and EV3A) by the StART-like domain of Ysp2p or any of the mammalian GramD1 proteins, supporting that they preferentially transport sterols.

The Osh4p protein also transfers PI(4)P, and *in vivo*, it transports sterol from the ER to the Golgi against a chemical gradient, by making use of energy stored in the PI(4)P gradient between these compartments and counter-exchanging sterol for the phosphoinositide (PIP) at the Golgi (de Saint-Jean *et al*, 2011; Moser von Filseck *et al*, 2015b). Another protein in the same oxysterol binding protein (OSBP) family, ORP8, similarly counter-exchanges PS for PI(4)P or PI(4,5)P₂ at ER–plasma membrane contact sites (Maeda *et al*, 2013; Chung *et al*, 2015; Ghai *et al*, 2017). As a first step in assessing whether any of the LAM/Ltc proteins might also use such a counter-exchange strategy, we examined whether they transfer either PI(4)P or PI(4,5)P₂, the two PIPs commercially available with a natural mammalian acyl chain distribution. We used the same FRET-based

assay described above for PS transfer, except with an NBD-labeled probe for PIPs rather than for PS (NBD-PH_{FAPP1}, the PH domain of FAPP1) (Moser von Filseck *et al*, 2015b). We did not observe either PI(4)P (Figs 3E and F, and EV3B) or PI(4,5)P₂ (Figs 3G and H, and EV3C) transfer by the StART-like domains of Ysp2p (Ysp2p_{S1}, Ysp2p_{S1S2}), GramD1a, or GramD1c, although we cannot exclude transport of other, untested PIPs. In contrast, the GramD1b StART-like domain transports PI(4,5)P₂ (Figs 3G and H, and EV3C), with comparatively weak activity for PI(4)P (Figs 3E and F, and EV3B). The polybasic sequence C-terminal to the GramD1b StART-like domain, which is not present in Ysp2p_{S1}, does not confer the ability to transport PI(4,5)P₂ since its truncation does not affect phosphoinositide transfer rates (Figs 3G and H, and EV3C) and since GramD1a, GramD1c, and Ysp2p_{S1S2}, which also have a C-terminal polybasic segment, did not transport the tested phosphoinositides effectively (Figs 3E–H and EV3B and C). The rate at which GramD1b transports PI(4,5)P₂ (~0.22 PIP molecules/min/GramD1b molecule) is comparable to PI(4,5)P₂ and PI(4)P transfer rates by ORP8 (residues: 370–809) (~0.31 PIPs/min/ORP8 molecule) and

Figure 3. Ligand specificity of Ysp2p and GramD1a-c.

- A Schematic of the PS/PIP transport assay. Donor liposomes L_D (93 mol% egg PC, 5 mol% PS/PIPs, and 2 mol% Rhod-PE 200 μM total lipid) were incubated with acceptor liposomes L_A (egg PC, 200 μM total lipid) and 250 nM NBD-C₂Lact/PH_{FAPP1}. After 4 min, LTP (1 μM final protein concentration) or buffer was added. Transfer of PS/PIPs between L_D and L_A liposomes leads to dequenching of the NBD fluorescence due to relocalization of NBD-C₂Lact/PH_{FAPP1} from L_D to L_A. For reference, the signal of a sample with PS/PIP in equilibrium between L_D (95.5 mol% egg PC, 2.5 mol% PS/PIP, 2 mol% Rhod-PE, 200 μM total lipid) and L_A (97.5 mol% egg PC, 2.5 mol% PS/PIP, 200 μM total lipid) was measured. After subtraction of the buffer reaction, the signal was normalized to the amount of PS/PIP present (μM) in L_A based on the signal of the equilibrium sample.
- B Cholesterol and PE transport assay. L_D liposomes (1 mM total lipid) were incubated with Ysp2p_{S1}, the StART-like domains of GramD1a-c (1 μM final protein concentration), or buffer. The transport reaction was started by the addition of heavy, sucrose filled L_A liposomes (1 mM total lipid) containing 5 mol% cholesterol or PE and spiked with 1 $\mu\text{Ci/ml}$ ³H cholesterol or 0.2 $\mu\text{Ci/ml}$ ¹⁴C PE, respectively. After 1 h, L_D and L_A liposomes were separated by centrifugation and the amount of radioactivity in each liposome population was determined. The signal was normalized to the amount of cargo lipid (in % of total cargo lipid) transferred to L_A after subtraction of the buffer control reaction (mean \pm SD, n = 3).
- C, D PS transport by Ysp2p_{S1} (blue for brain PS, light blue for DPPS), the StART-like domains of GramD1a/b/c (purple, red and orange respectively), or, as a positive control, the known PS transporter ORP8 (gray, residues 370–809; Maeda *et al*, 2013; Chung *et al*, 2015; 1 μM final protein concentration). Addition of 5% PI(4,5)P₂ to the acceptor liposomes increased ORP8 PS transfer rate (black) (as reported in Ghai *et al*, 2017). For Ysp2p_{S1}, we tested transfer of both brain PS and DPPS, which has shorter acyl chains. This alleviated concerns that even while not transferring brain PS, the yeast construct Ysp2p_{S1} might transfer PS species abundant in yeast, with shorter fatty acid moieties than brain PS. The dashed black line represents PS equilibrium between L_D and L_A. Mean of three independent experiments. For mean \pm SD, see Fig EV3A. (D) Initial PS transfer rates (V_i, mean \pm SD, n = 3).
- E, F PI(4)P transport by Ysp2p_{S1} (blue, light blue for diC16 lipid, whose acyl chain composition more closely resembles that in yeast), Ysp2p_{S1S2} (steel blue), the StART-like domains of GramD1a-c (purple, red and orange, respectively), or Osh4p (black) (1 μM final protein concentration). The dashed black line represents PI(4)P equilibrium between L_D and L_A. Mean of three independent experiments. For mean \pm SD, see Fig EV3B. (F) Initial PI(4)P transfer rates (V_i, mean \pm SD, n = 3).
- G, H PI(4,5)P₂ transport by Ysp2p_{S1} (blue, light blue for diC16 lipid, whose acyl chain composition more closely resembles that in yeast), Ysp2p_{S1S2} (steel blue), the StART-like domains of GramD1a-c (purple, red, and orange, respectively), GramD1b_{short} (green), or ORP8 (gray) (1 μM final protein concentration). The dashed black line represents PI(4,5)P₂ equilibrium between L_D and L_A. Mean of three independent experiments. For mean \pm SD, see Fig EV3C. (H) Initial PI(4,5)P₂ transfer rates (V_i, mean \pm SD, n = 3).

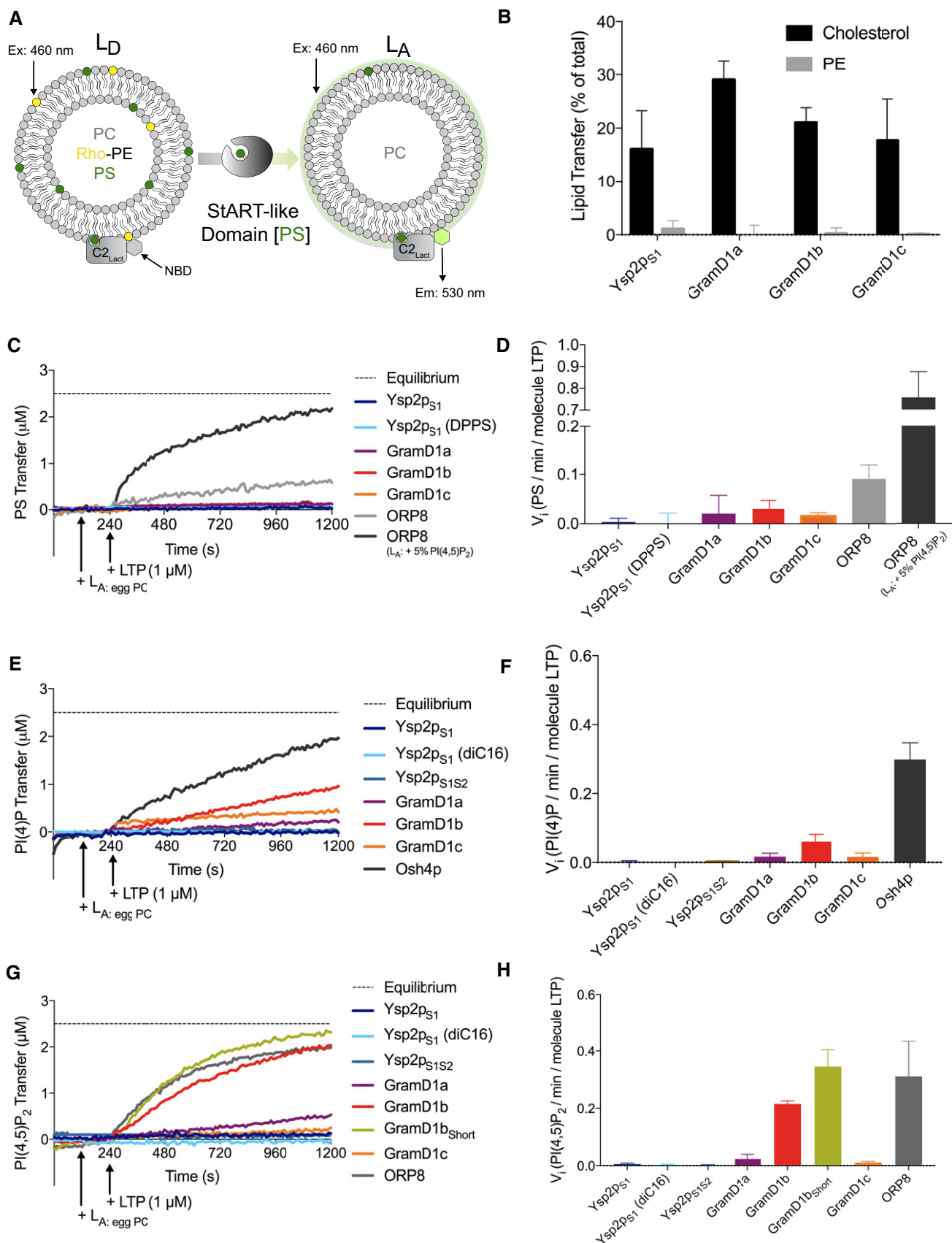


Figure 3.

Osh4p (~0.30 PIPs/min/Osh4p molecule), respectively, under the same conditions (Fig 3E–H). GramD1b might transfer other untested PIPs (e.g., PI3P or PI(3,5)P₂ if it localizes to the endolysosomal system) even more efficiently, just as it transfers PI(4,5)P₂ more rapidly than PI(4)P. Further, a more physiological membrane composition may accelerate phosphoinositide transport just as it accelerates sterol transport.

These results suggest the intriguing possibility that GramD1b might function in phosphoinositide transport and could employ a counter-exchange mechanism. The physiological relevance of phosphoinositide transfer by GramD1b will need to be further evaluated once its localization in cells, and the sterol and phosphoinositide composition of donor and acceptor membranes, is better understood.

StART-like domains adopt a truncated α/β helix-grip fold

For insights as to how the LAM/Ltc StART-like domain proteins, and by extension the related StART domain proteins, bind sterols, we crystallized a fragment of *S. cerevisiae* Ysp2p containing the first of two StART-like domains (Ysp2p_{S1}, residues 851–1,017). The construct is identical to that used in the DHE transfer experiments above. The protein was expressed in *E. coli*, purified, and crystallized in the presence of a twofold molar excess of ergosterol, and its structure was solved by the single anomalous wavelength dispersion method (SAD) (Hendrickson, 1991) using data from a selenomethionine-substituted crystal. The final model contains four molecules of the StART-like domain in the asymmetric unit and includes all residues from 851 to 1,016, except for residue 1,016 in one of the copies and 851 in two others. Two of the molecules showed non-peptide density in their ligand binding cavity corresponding to a bound ergosterol moiety. The final model additionally contains 709 water molecules. The refined structure has $R_{\text{work}}/R_{\text{free}}$ values of 16.1/20.1% and good stereochemistry (Table 1).

Ysp2p_{S1} folds into a cup-shaped structure, whose walls comprise a six-stranded β -sheet (β 1– β 6) and a three-helix bundle (α 1– α 3) (Fig 4A and B). Superposition of Ysp2p_{S1} with the StART domain of StARD3 (PDB ID: 5i9j, 3.0 Å RMSD over 131 C α atoms) shows that the StART-like fold is a truncated version of the canonical α/β helix-grip fold adopted by StART domain proteins (Fig 4C). Missing are the α -helix and adjacent two β -strands present at the N-terminus of the StART domains, including in StARD3 (Fig 4C). One of the strands at the edge of the StART β -sheet (β 4) is replaced by a random coil segment in Ysp2p, where two proline residues (P893 and P895) interfere with hydrogen bonding interactions to the adjacent β -strand (which is β 2 in Ysp2p_{S1} or β 5 in StART domains). Another difference is in the positioning of loop Ω 2 connecting β 4 with β 5 in Ysp2p_{S1} (or β 7 with β 8 in StARD3) (Fig 4C). In the StART domains, this loop packs against the β -sheet outside the cavity, whereas in the Ysp2p StART-like domain, it forms part of the wall defining the cavity.

Comparison of the apo- and sterol-bound forms of Ysp2p_{S1}

A superposition of the ligand-bound and ligand-free copies of Ysp2p_{S1} reveals a conformational change upon sterol binding (Fig 5A). In the apo form of Ysp2p_{S1}, the opening to the sterol

Table 1. Crystallographic statistics.

Data collection	
Space group	P 1 2 ₁ 1
Unit cell dimensions (a, b, c in Å; α , β , γ in °)	67.59, 63.56, 77.54, 90, 103.58, 90
Wavelength (Å)	0.9792
Resolution (Å)	75.4–1.89 (1.96–1.89)
R_{merge}	0.107 (0.338)
I/σ	30.4 (6.4)
Completeness (%)	94.4 (71.4)
Redundancy	20.4 (10.1)
Refinement	
Resolution (Å)	75.4–2.0
No. of unique reflections	42,580
$R_{\text{work}}/R_{\text{free}}$ (%)	16.11/20.12
No. of non-hydrogen atoms	
Protein	5,272
Water	709
Ligands	58
Average B (Å ²)	
Protein	15.37
Water	26.38
Ligands	21.58
Rmsd	
Bond length (Å)	0.008
Bond angle (°)	0.91
Ramachandran plot	
Favored (% residues)	98.3
Allowed (% residues)	1.7
Disallowed (% residues)	0

binding site is large enough to allow binding and release of the ligand, assuming that the side chain of K910 moves into the position observed in the ergosterol-bound conformation (Fig 5A). Upon ligand binding, loops Ω 1 and Ω 2 (localized between β 2 and β 3 and between β 4 and β 5, respectively), the N-terminal end of helix α 3, and the loop connecting β 6 with α 3 move to partially close off the opening of the sterol binding cavity (Fig 5A). While the displacement is minor for the other structural elements (< 1.6 Å), the tip of Ω 1 moves by ~6 Å closer to helix α 3. As a result, the ligand is largely shielded from the aqueous environment.

The 3-hydroxyl group of ergosterol is coordinated by a water network at the base of the ligand binding cavity

Ergosterol is bound by two of the copies of Ysp2p_{S1} in the asymmetric unit (Fig 5B) and occupies the portion of the ligand binding cavity closest to the entrance (Fig 5C). Residues lining this portion of the cavity are hydrophobic as are residues in the Ω 1 (L912, I916, P918) and Ω 2 (V949, F955) loops (Fig 5E) which also interact with the

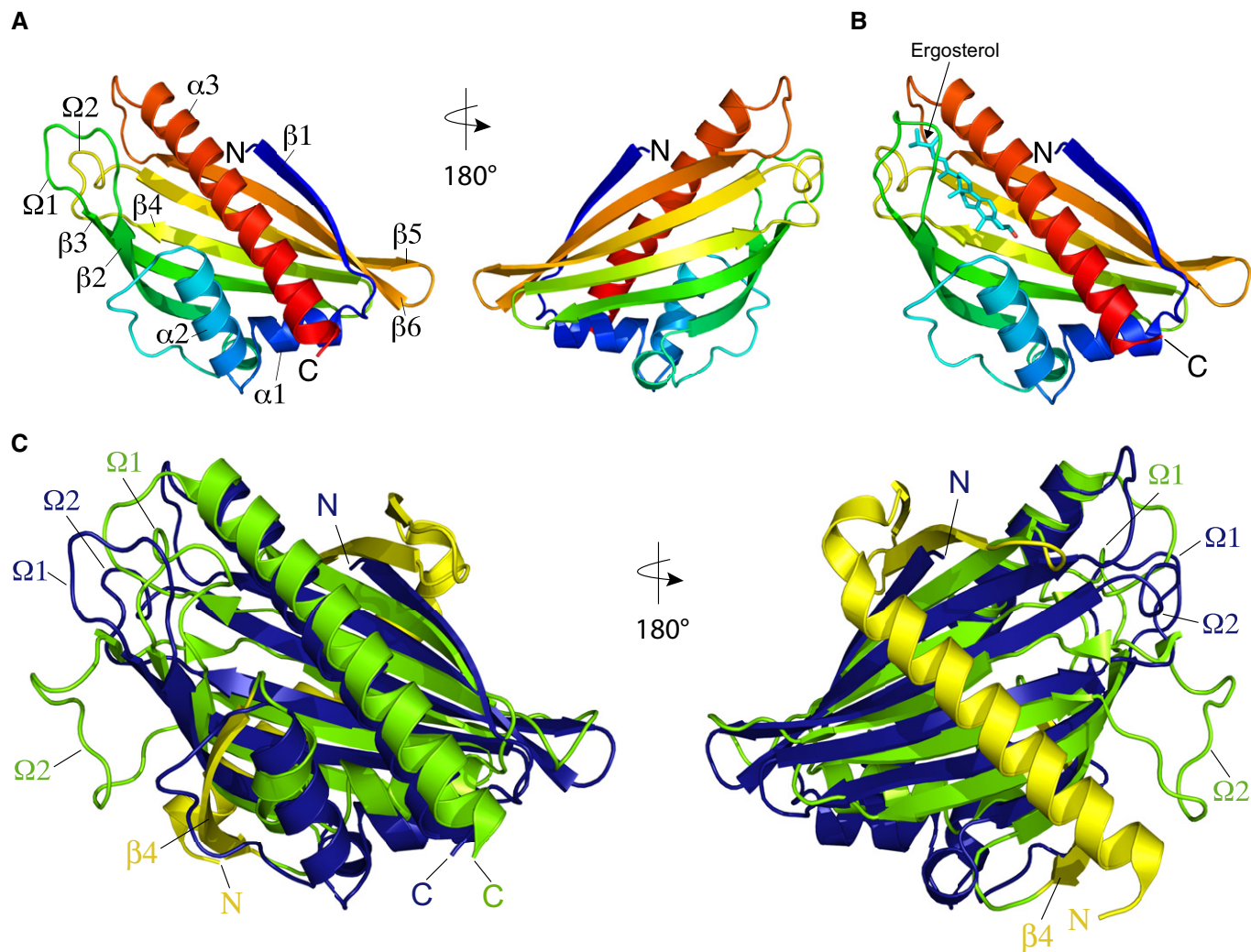


Figure 4. Crystal structure of the apo-bound and ergosterol-bound forms of Ysp2p StART-like domain 1.

A Structure of apo Ysp2p StART-like domain 1 (Ysp2p_{S1}) in cartoon representation colored blue to red from N-terminus to C-terminus.

B Structure of Ysp2p_{S1} (cartoon representation), colored blue to red from N-terminus to C-terminus, bound to ergosterol (cyan, stick representation).

C Superposition of apo Ysp2p_{S1} (dark blue) and the StART domain of StARD3 (PDB ID: 5I9J, RMSD 3.0 Å over 131 C α atoms), both in cartoon representation. Structural elements of StARD3 not conserved in Ysp2p are colored yellow while conserved elements are green.

sterol, and they are conserved with respect to Ysp2p from different fungi (Fig EV4) as well as to LAM/Ltc StART-like domains more generally (Fig 5D and E). The ergosterol is oriented “head down”, so that its 3-hydroxyl group is furthest from the entrance to the cavity (Fig 5C). Intriguingly, the 3-hydroxyl group of ergosterol does not form any direct hydrogen bonds with Ysp2p and instead interacts with four water molecules, at distances of ~2.5, ~3.5, 3.8, and ~3.9 Å, that are part of a larger, well-ordered water network occupying the bottom third of the cavity (Fig 5C). The position of these water molecules is preserved in all copies of Ysp2p_{S1} independent of whether ergosterol is bound or not (in the ligand-free Ysp2p_{S1}, additional waters occupy the ergosterol binding site). The water network is coordinated by a cluster of polar residues (Y872, Y879, Q886, N888, Y906, Y908, K910, S942, T1002, T1003) and an aspartate (D927) at the bottom of the cavity (Fig 5C). Of these residues, the ability to

coordinate water molecules is highly conserved across different species, as well as in the LAM/Ltc family as a whole, at the positions corresponding to Q886, Y908, and D927 in Ysp2p (Figs 5D and E, and EV4).

Mutational analysis validates the sterol binding site in Ysp2p_{S1} and GramD1b

Next, to validate the sterol binding site identified from the crystal structure, we designed mutations in the hydrophobic cavity of Ysp2p_{S1} to interfere with sterol binding and tested their effects on sterol transfer rates (Fig 6A). For the mutations, we replaced smaller residues with bulkier ones or exchanged hydrophobic and hydrophilic residues or reversed their charges. We found that mutations in the $\Omega 1$ loop ($\Omega 1_{\text{mut}}$: L912S/I916S/P918S), the $\Omega 2$ loop

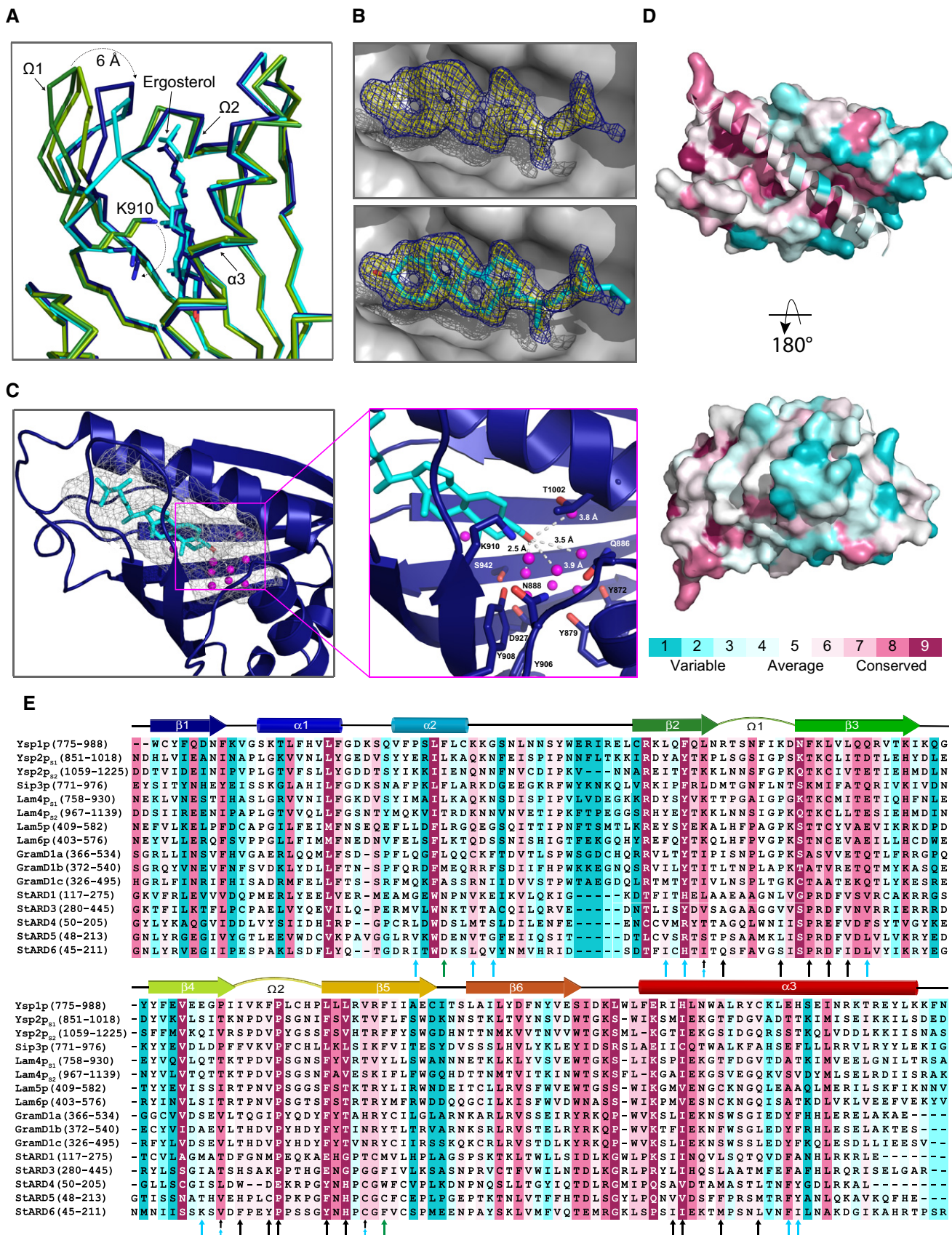


Figure 5.

Figure 5. Structural basis for sterol recognition by StART-like domains.

- A Superposition of the apo-bound and ergosterol-bound copies of Ysp2p_{S1} (ribbon representation) found in the asymmetric unit of the Ysp2p_{S1} crystal. The apo-bound form copies are in green and lime, and the ligand-bound copies and their respective ergosterol moieties (stick representation) are in blue and cyan. The $\Omega 1$ loop moves -6 Å closer (dashed line) to $\alpha 3$ upon ergosterol binding, thereby partially closing the opening to the ligand binding site.
- B Ergosterol (cyan, stick representation) placed in unbiased positive electron density (mFo-DFc map, $\sigma = 3.0/2.0$, dark blue/yellow, mesh) in the binding cavity of Ysp2p_{S1} (light gray, surface representation). Helix $\alpha 3$ has been removed for better visibility.
- C View of the ligand binding cavity (gray, mesh) of Ysp2p_{S1} (dark blue, cartoon). A network of water molecules (magenta dots) occupies the bottom of the Ysp2p_{S1} cavity. Ergosterol (cyan, stick representation) binds "head down" in the upper portion of the Ysp2p_{S1} cavity. There are no direct hydrogen bonds between the ergosterol 3-OH group and the protein. Instead, the 3-OH group interacts with four well-ordered water molecules (magenta) at 2.5, 3.5, 3.8, and 3.9 Å distance (dashed white lines). Side chains are shown for residues coordinating water molecules at the bottom of the cavity.
- D Surface representation of Ysp2p_{S1} color-coded by sequence conservation in the StART-like family and sterol transporters in the StARD family according to the ConSurf server (Landau et al, 2005; Ashkenazy et al, 2016). Helix $\alpha 3$ in cartoon representation for better visibility of the ligand binding cavity.
- E Sequence and structure-based alignment of the yeast and human StART-like domains and sterol transporters in the StARD family. Color-coded by sequence conservation as in Fig 4D. The secondary structure of Ysp2p_{S1} is shown above (color-coded blue to red from N-terminus to C-terminus as in Fig 3A and B). Residues with side chains lining the ligand binding cavity of Ysp2p_{S1} are marked with arrows (black arrows: residues lining the ergosterol binding site, blue arrows: residues coordinating water molecules in the cavity, green arrows: other).

($\Omega 2_{\text{mut}}$: V949T/F955Y), or the upper portion of the cavity (T921D, N946E), where wild-type residues are in van der Waals contact with ergosterol, abrogated sterol transfer (Figs 6B and EV5A). Conversely, mutations nearer (S942E) or at the base of the cavity (D927L, Q886L/Y908F, D927E), which is occupied by water in the crystal structure, had a small or no effect on sterol transfer activity (Figs 6B and EV5A). Thus, the mutational analysis is consistent with sterol binding in the upper portions of the hydrophobic cavity and highlights the importance of the $\Omega 1$ and $\Omega 2$ loop interactions for lipid binding.

Based on a sequence alignment with Ysp2p (Fig 5E), we made corresponding mutations in GramD1b and assayed the mutants for sterol transfer activity. We again found that mutations in the $\Omega 1$ loop ($\Omega 1_{\text{mut}}$: L434S/L438S/P440S) or the upper portions of the cavity (A443D, T469D) had the largest effect on sterol transfer rates (Figs 6C and EV5B), whereas the effects of mutations nearer (A465L) or at the base of the cavity (Q449L, R406L/Y430F) were smaller (Figs 6C and EV5B). Although they did affect sterol transfer, the mutations in the $\Omega 2$ loop ($\Omega 2_{\text{mut}}$: V472T/F478Y) had a smaller effect for GramD1b than for Ysp2p_{S1}. A plausible explanation is that the $\Omega 2$ loops of Ysp2p_{S1} and GramD1b adopt slightly different conformations, and, in the absence of a sterol-bound GramD1b structure, we may not have mutated the residues in GramD1b in closest contact with sterol. Overall, however, the mutational analysis indicates that the sterol binding site identified from the Ysp2p_{S1} structure is conserved in GramD1b and likely other LAM/Ltc StART-like domains.

To obtain insights as to how GramD1b might solubilize PIPs, we further examined the effect of the GramD1b mutations on PI(4,5)P₂ transfer. We found that mutations in the $\Omega 1$ and $\Omega 2$ loops reduced PI(4,5)P₂ transfer rates (Figs 6D and EV5C), as with sterol transfer, and several mutations near the top or middle of the cavity (A443D, T469D, A465L) altered transfer kinetics (Fig EV5C). These mutants displayed a fast initial rate, but then transfer plateaued before equilibrium was reached. A likely explanation is that the initial rate corresponds to a lipid extraction step, which is followed by inefficient delivery to acceptor membranes (Fig EV5C). Different from their effect on sterol transfer, mutations at or near the base of the cavity impacted phosphoinositide transfer. The R406L/Y430F mutation increased PI(4,5)P₂ transfer rates, by ~ 3 -fold (Fig 6D), and the Q449L mutation showed altered transfer kinetics (Fig EV5C). The finding that mutations nearer or at the base of the cavity affected

PI(4,5)P₂ but not sterol transfer suggests that, different from sterol, PI(4,5)P₂ occupies the entire cavity.

Implications for sterol binding by StART domain proteins

In metazoa, proteins in the StART domain family—StARD1, StARD3, StARD4, StARD5 (Clark, 2012; Alpy & Tomasetto, 2014; Letourneau et al, 2015)—play a major role in sterol transport. How these proteins interact with sterol, however, remains unknown as crystal structures are only available for their apo-bound form (Tsujishita & Hurley, 2000; Romanowski et al, 2002; Thorsell et al, 2011; Iaea et al, 2015; Horvath et al, 2016). The depth of the cavity in these StARD proteins is similar to that in Ysp2p_{S1}, and polar residues which can coordinate waters also line the base of the cavity. These waters are modeled in the StARD3 and StARD4 structures, which were determined at high resolution (Tsujishita & Hurley, 2000; Romanowski et al, 2002; Iaea et al, 2015; Horvath et al, 2016). Thus, given the evolutionary relationship between StART and StART-like domain transporters, it is probable that the manner in which the StART proteins bind sterol will be similar to Ysp2p_{S1} and the LAM/Ltc StART-like domains: The sterol will bind near the opening of the cavity, with water occupying the cavity base. This differs from modeling predictions that sterol binds at the bottom of the cavity (Tsujishita & Hurley, 2000; Mathieu et al, 2002; Murcia et al, 2006; Thorsell et al, 2011; Letourneau et al, 2015). StART domain structures (PDB IDs: 3p0L (StARD1), 5i9j/3fo5 (StARD3/MLN64), 1jss/5brl (StARD4), 2r55 (StARD5), 2pso (StARD13)) show the proteins in a "closed" form, with the $\Omega 1$ loop closing the lipid binding cavity almost completely off from solvent. Most likely, the loop can also adopt an open conformation, allowing sterol to enter or exit the cavity as in Ysp2p_{S1}. When sterol is bound, the $\Omega 1$ loop would close or close partially as in the Ysp2p_{S1} structure. If sterol binding by the StARD proteins is similar to what is observed in the Ysp2p_{S1} structure, it seems unlikely that sterol uptake or delivery involves partial protein unfolding or melting, as previously speculated (Bose et al, 2000; Mathieu et al, 2002; Baker et al, 2005; Roostae et al, 2009; Lavigne et al, 2010).

The StART and related StART-like domain proteins, all sharing a similar cup-shaped fold, solubilize a diverse set of lipids, including glycerolipids as well as the smaller sterols. As a solution for accommodating lipids of different size in similarly sized

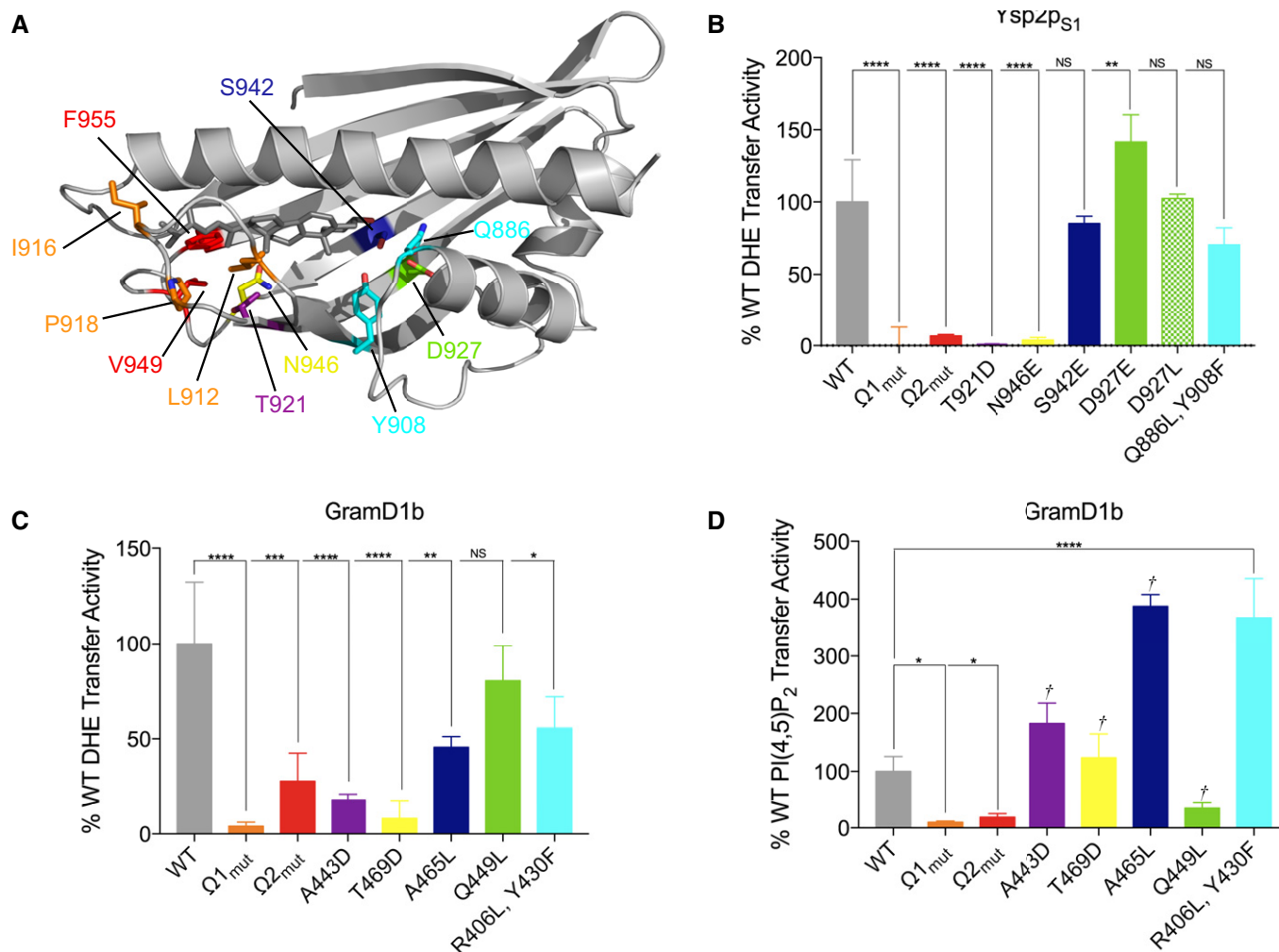


Figure 6. Mutational analysis of the ligand binding site in Ysp2p_{S1} and GramD1b.

A Cartoon representation of ergosterol (dark gray)-bound Ysp2p_{S1} (light gray). Side chains are shown for residues mutated to interfere with lipid transfer activity.
 B DHE transfer rates of Ysp2p_{S1} mutants relative to WT activity. For transfer curves (mean ± SD, n = 3), see Fig EV5A. Mutants are color-coded as indicated in (A) (V_i, mean ± SD, n = 3. *P < 0.05, **P < 0.01, *P < 0.001, ****P < 0.0001, NS: not significant). ANOVA with Dunnett's multiple comparisons test.
 C DHE transfer rates of Ysp2p_{S1} mutants relative to WT activity. For transfer curves (mean ± SD, n = 3), see Fig EV5B. Mutants are color-coded corresponding to their Ysp2p counterparts as indicated in (A) (V_i, mean ± SD, n = 3. *P < 0.05, **P < 0.01, ***P < 0.001, ****P < 0.0001, NS: not significant). ANOVA with Dunnett's multiple comparisons test.
 D PI(4,5)P₂ transfer rates of the StART-like domain of GramD1b mutants relative to WT activity. For transfer curves (mean ± SD, n = 3), see Fig EV5C. Mutants are color-coded corresponding to their Ysp2p counterparts as indicated in (A). †: These mutants displayed altered transfer kinetic with a fast initial step, likely corresponding to lipid extraction only, followed by inefficient delivery to acceptor membranes (Fig EV5C). The rates calculated for these mutants should not be directly compared to the WT rates (V_i, mean ± SD, n = 3. *P < 0.05, **P < 0.01, *P < 0.001, ****P < 0.0001, NS: not significant). ANOVA with Dunnett's multiple comparisons test.

cavities, LAM/Ltc and probably the related StART domains bind sterols in the “upper” portion of the cavity while the base of the cavity is filled with water molecules. Larger lipids like PC or ceramide, on the other hand, also occupy the base of the cavity (Roderick *et al*, 2002; Tilley *et al*, 2004; Vordtriede *et al*, 2005; Kudo *et al*, 2008). In Ysp2p_{S1} and so presumably in other StART-like and the StART domains, sterol binds in a “heads down” fashion, with the 3-hydroxyl group interacting with a water network at the bottom of the ligand binding cavity. This seems to be a common mode of sterol binding by lipid transfer proteins as members of the Osh/OSBP family interact with sterol similarly (Im *et al*, 2005; Koag *et al*, 2013).

Materials and Methods

Protein expression and purification

All recombinant proteins were expressed in *E. coli* BL21(DE3) as PreScission protease cleavable GST-fusion proteins. Cells were grown at 37°C to an OD₆₀₀ of 0.6, when expression was induced by the addition of isopropyl β-D-1-thiogalactopyranoside (0.3 mM) and the temperature was lowered to 18°C. Cells were harvested 20 h after induction. Selenomethionine-substituted Ysp2p_{S1} was expressed similarly according to Budisa *et al* (1995). Cells were resuspended in buffer A (20 mM Tris pH 7.5, 500 mM NaCl, 1 mM

Tris(2-carboxyethyl)phosphine (TCEP), 20% glycerol), supplemented with protease inhibitors [phenylmethylsulfonyl fluoride at 1 mM and “complete ethylenediaminetetraacetic acid (EDTA)-free”, Roche], and lysed at 4°C using a cell disruptor (Avestin). The cell lysate was cleared by centrifugation, and the GST-fusion protein was isolated by affinity chromatography using glutathione–sepharose 4B resin (GE Life Science). The proteins were eluted from the resin by overnight on-column cleavage with PreScission protease at 4°C. Proteins were further purified by size exclusion chromatography (Superdex S75 10/300 increase) using buffer A or, for crystallization experiments, buffer B (20 mM Tris pH 7.5, 150 mM NaCl, 2 mM TCEP). Eluted protein was concentrated and either used directly in crystallization experiments or aliquoted and flash-frozen for later use in biochemical assays.

NBD-labeled PH_{FAPP} and C₂Lact were prepared according to Moser von Filseck *et al* (2015a,b), respectively.

Lipids

Egg PC (Cat # 840051), brain PI(4)P (Cat # 840045), brain PI(4,5)P₂ (Cat # 840046), brain PS (Cat # 840032), liver PE (Cat # 840026), DNS-PE (Cat # 810330), Rhod-PE (Cat # 810150), DHE (Cat # 810253), DOPC (Cat # 850375), DGS-NTA(Ni) (Cat # 790404), and cholesterol (Cat # 700000) were purchased from Avanti Polar Lipids. Ergosterol (Cat # 02101649) was purchased from MP Biomedicals. 1,2-Dipalmitoyl-sn-glycero-3-phosphoserine (DPPS, Cat # L-3116), diC16 PI(4)P (Cat # P-4016), and diC16 PI(4,5)P₂ (Cat # P-4516) were purchased from Echelon Bioscience. Radiolabeled cholesterol (24,25-³H) (Cat # ART1987) and PE (L- α -1-palmitoyl-2-arachidonyl, arachidonyl-1-14C) (Cat # ARC 0855) were purchased from American Radiolabeled Chemicals, Inc.

Liposome preparation

Lipids were mixed in the desired molar ratios, and the organic solvent was removed using nitrogen gas. The resulting lipid films were hydrated for 1 h at 37°C or at 85°C for liposomes containing diC16 lipids with 50 mM HEPES, pH 7.2, and 120 mM K-acetate (HK buffer) to produce multilamellar liposomes. After five freeze/thaw cycles with liquid nitrogen, the liposomes were extruded through polycarbonate filters (100 nm pore size) using a mini-extruder (Avanti Polar Lipids). To obtain “heavy” sucrose filled liposomes, the buffer additionally contained 0.75 M sucrose and the liposomes were not extruded after the freeze/thaw step. Prior to use, the heavy liposomes were washed 2× with HK buffer and finally resuspended in HK buffer at the desired concentration.

PE and cholesterol transport assay

A 55 μ l solution of L_A liposomes (PC, 1 mM final concentration) and the individual proteins (1 μ M final concentration) was mixed with 45 μ l “heavy” sucrose filled L_D liposomes (1 mM final concentration). L_D liposomes contained 95 mol% egg PC and either 5 mol% cholesterol or PE and were spiked with 1 μ Ci/ml ³H cholesterol or 0.2 μ Ci/ml ¹⁴C PE, respectively. The reaction was incubated at 25°C for 1 h under constant rotation to avoid sedimentation of the L_D liposomes. After 1 h, L_A and L_D liposomes were separated by centrifugation at 16,100× *g* for 15 min. The radioactivity in the

pellet (P) and supernatant (S) was detected separately by scintillation counting. The percentage of total lipid transferred Δ Lipid was calculated using the following formula: Δ Lipid = $100 \cdot (S)/(S + P) - 100 \cdot (S_0)/(S_0 + P_0)$. P₀ and S₀ correspond to the activity measured in the pellet and in the supernatant of a reaction contacting no LTPs, respectively.

DHE transport assay

Donor liposomes L_D (640 μ l, 200 μ M final lipid concentration) containing 92.5 mol% PC, 5 mol% DHE, and 2.5 mol% DNS-PE were incubated at 30°C under constant stirring. After 2 min, 80 μ l acceptor liposomes L_A (200 μ M, final lipid concentration) were injected. After 4 min, the transfer reaction was started by addition of 80 μ l of the respective protein (1 μ M final protein concentration) or HK buffer. DHE transfer from PM-like donor liposomes (L_{PM}) to ER-like acceptor liposomes (L_{ER}) was carried out similarly, except that L_{PM} liposomes contained 65% egg PC, 17.5% PE, 10% PS, 5% DHE, and 2.5% DNS-PE; L_{ER} liposomes contained 78% DOPC, 20% PE, and 2% DGS-NTA(Ni); and that the final LTP concentration was 0.1 μ M. DHE equilibrates quickly between the inner leaflet and outer leaflet of liposomes with $t_{1/2}$ of transbilayer movement reported to be between ~1 s (Steck *et al*, 2002) in red blood cell bilayers at 37°C and 20–50 s in egg PC and DOPC liposomes at 10°C (John *et al*, 2002). Accordingly, the entire DHE pool of 10 μ M is accessible to the transfer proteins. DHE transfer was monitored by measuring DNS fluorescence at 495 nm upon excitation of DHE at 310 nm. The amount of DHE transferred from L_D to L_A liposomes (Δ DHE) at a time point *t* was calculated using following formula: Δ DHE_{*t*} = Δ DHE_{eq}(F_{*t*}-F_{*c*})/(F_{eq}-F_{*c*}). Δ DHE_{eq} is the difference in DHE content between liposomes L_A at *t* = 0 and at equilibrium (5 μ M), F_{*t*} is the fluorescent signal at *t*, F_{*c*} is the signal of a control reaction (with HK buffer added to the liposomes instead of protein solution) at *t*, F_{eq} is the signal of a sample at equilibrium at *t*. F_{eq}, the fluorescence signal of a sample at DHE equilibrium, was determined by measuring a solution (800 μ l) containing 200 μ M L_{Deq} (95 mol% PC, 2.5 mol% DHE, 2.5 mol% DNS-PE) and L_{Aeq} (97.5 mol% PC, 2.5 mol% DHE). Transfer rates were calculated by determining the slope of the initial linear portion of the transfer reaction (*n* = 3).}

PIP and PS transport assay

Donor liposomes L_D (640 μ l, 200 μ M final lipid concentration) containing 93 mol% PC, 2 mol% Rhod-PE, and either 5 mol% PI(4)P, PI(4,5)P₂ or PS were incubated with 250 nM NBD-PH_{FAPP1} (PIPs) or NBD-C₂Lact (PS) at 30°C under constant stirring. After 2 min, 80 μ l acceptor liposomes L_A (egg PC, 200 μ M final lipid concentration) were added. After 4 min, the transfer reaction was started by injecting 80 μ l of the individual proteins (1 μ M final concentration) or buffer. Since only PIPs/PS in the outer membrane leaflets are accessible, the effective volume concentration of PIPs/PS is 2.5 μ M. The signal of NBD-PH_{FAPP1}/C₂Lact corresponds to the distribution of PIPs/PS between L_D and L_A liposomes. PIP/PS transfer was monitored by measuring NBD fluorescence at 535 nm upon excitation at 460 nm. The amount of PS or PIP (Δ PX) transferred from L_D to L_A liposomes at a time point *t* was calculated using the following

formula: $\Delta PX_t = \Delta PX_{eq}(F_t - F_c)/(F_{eq} - F_c)$. ΔPX_{eq} (2.5 μ M) is the difference in PIP/PS content of L_A liposomes at $t = 0$ and at equilibrium, F_t is the fluorescent signal at t , F_c is the signal of a control reaction (with HK buffer added to the liposomes instead of protein solution) at t , F_{eq} is the signal of a sample at equilibrium at t . F_{eq} was determined by measuring a solution (800 μ l) containing 200 μ M L_{Deq} (95 mol% PC, 2.5 mol% PIP/PS, 2.5 mol% Rhod-PE), L_{Aeq} (97.5 mol% PC, 2.5 mol% PIP/PS), and 250 nM NBD-PH_{Fapp} (PIP) or NBD-C2_{Lact} (PS). Transfer rates were determined by calculating the slope of the initial linear portion of the transfer reaction. The average acyl chain length of glycerol phospholipids in yeast is shorter than in mammalian cells (Ejsing *et al*, 2009). To test whether acyl chain length had an influence on the lipid transfer activity of Ysp2p_{S1}, we also performed the PS and PIP transfer assays with lipids comprising dipalmitoyl (16:0–16:0) acyl chains (DPPS and diC16 PIPs), which are shorter than those in the brain lipids.

Protein crystallization, data collection, and structure determination

Initial Ysp2p crystals (Ysp2p_{S1}: residues 851–1,017, at 18 mg/ml concentration) were grown in the presence of a twofold molar excess of ergosterol using the hanging drop vapor diffusion method at 22°C against a reservoir solution of 32.5% PEG 3350, 0.1 M sodium acetate (pH 4.9), 0.2 M ammonium acetate. The resulting crystals were crushed and used as microseeds under the same conditions to obtain large single crystals for data collection. Crystals were grown for 10–14 days to reach their final size after which they were briefly incubated in mother liquor supplemented with 20% ethylene glycol for cryoprotection and flash-frozen. Diffraction data were collected at beamline NE-CAT 24-ID-E at Argonne National Laboratories (APS) and processed using XDS (Kabsch, 1993). The structure of Ysp2p was determined using the single-wavelength anomalous dispersion (SAD) method at the selenium edge with data from a selenomethionine-substituted crystals (Hendrickson, 1991). We identified the selenium positions, calculated experimental phases and density-modified maps, and built an initial model using the phenix AutoSol pipeline (Adams *et al*, 2010). After initial simulated annealing (torsion angle) in phenix.refine (Adams *et al*, 2010), the model was refined to 2.0 Å resolution by multiple cycles of manual model rebuilding in coot (Emsley *et al*, 2010) followed by positional and individual B-factor refinement with phenix.refine using non-crystallographic symmetry (NCS) torsion angle restraints (Adams *et al*, 2010). Figures were made using PyMOL (The PyMOL Molecular Graphics System).

Bioinformatics

The multiple sequence and structure alignment of the LAM/Ltc proteins and human StARD family members implicated in cholesterol transport was generated using the PROMALS3D server (Pei & Grishin, 2014). Ysp2p_{S1} homologues (150 sequences, max/min sequence identity 95%/35%) were identified using HMMER and aligned with CLUSTALW using the ConSurf server (Landau *et al*, 2005; Ashkenazy *et al*, 2016). Conservation scores were calculated and projected onto the

crystal structure of Ysp2p_{S1} using the ConSurf server (Landau *et al*, 2005; Ashkenazy *et al*, 2016).

Statistics

Statistical analysis of lipid transfer experiments was performed with GraphPad Prism 7.0c. For comparing the mean of two groups, we used an unpaired, two-tailed *t*-test. To compare the mean of multiple groups to the mean of a control group, we used one-way ANOVA followed by Dunnett's multiple comparisons method. Brown–Forsythe test was used to test variance similarity.

Data availability

The accession number for the coordinates and structure factors for Ysp2p reported in this paper is PDB: 6CAY.

Expanded View for this article is available online.

Acknowledgements

X-ray data were collected at Northeastern Collaborative Access Team beamline 24-ID-E, funded by National Institute of General Medical Sciences (P41 GM103403), and we are grateful to NE-CAT staff for their assistance. Additionally, we thank Nikit Kumar for help with bioinformatics. This work was funded by the NIH (R01GM80616 to KMR; R37GM097432 and R01GM106019 to JN) and by an NSF Graduate Research Fellowship to DPV. We thank Pietro De Camilli for the plasmid encoding GST-ORP8 (residues 370–809).

Author contributions

FAH, DPV, and KMR designed the experiments. FAH and DPV carried out the experiments under the supervision of FAH and KMR. FAH and KMR wrote the manuscript with input from the other authors, and DPV assembled the figures. JN identified a soluble Ysp2p construct initially used for protein expression.

Conflict of interest

The authors declare that they have no conflict of interest.

References

- Adams PD, Afonine PV, Bunkoczi G, Chen VB, Davis IW, Echols N, Headd JJ, Hung LW, Kapral GJ, Grosse-Kunstleve RW, McCoy AJ, Moriarty NW, Oeffner R, Read RJ, Richardson DC, Richardson JS, Terwilliger TC, Zwart PH (2010) PHENIX: a comprehensive Python-based system for macromolecular structure solution. *Acta Crystallogr D Biol Crystallogr* 66: 213–221
- Alpy F, Tomasetto C (2014) START ships lipids across interorganelle space. *Biochimie* 96: 85–95
- Ashkenazy H, Abadi S, Martz E, Chay O, Mayrose I, Pupko T, Ben-Tal N (2016) ConSurf 2016: an improved methodology to estimate and visualize evolutionary conservation in macromolecules. *Nucleic Acids Res* 44: W344–W350
- Baker BY, Yaworsky DC, Miller WL (2005) A pH-dependent molten globule transition is required for activity of the steroidogenic acute regulatory protein, StAR. *J Biol Chem* 280: 41753–41760
- Bigay J, Antonny B (2012) Curvature, lipid packing, and electrostatics of membrane organelles: defining cellular territories in determining specificity. *Dev Cell* 23: 886–895

- Bose HS, Baldwin MA, Miller WL (2000) Evidence that StAR and MLN64 act on the outer mitochondrial membrane as molten globules. *Endocr Res* 26: 629–637
- Budisa N, Steipe B, Demange P, Eckerskorn C, Kellermann J, Huber R (1995) High-level biosynthetic substitution of methionine in proteins by its analogs 2-aminohexanoic acid, selenomethionine, telluromethionine and ethionine in *Escherichia coli*. *Eur J Biochem* 230: 788–796
- Chung J, Torta F, Masai K, Lucast L, Czaplá H, Tanner LB, Narayanaswamy P, Wenk MR, Nakatsu F, De Camilli P (2015) INTRACELLULAR TRANSPORT. PI4P/phosphatidylserine countertransport at ORP5- and ORP8-mediated ER-plasma membrane contacts. *Science* 349: 428–432
- Clark BJ (2012) The mammalian START domain protein family in lipid transport in health and disease. *J Endocrinol* 212: 257–275
- Drin G, Moser von Filseck J, Copic A (2016) New molecular mechanisms of inter-organelle lipid transport. *Biochem Soc Trans* 44: 486–492
- Ejsing CS, Sampaio JL, Surendranath V, Duchoslav E, Ekroos K, Klemm RW, Simons K, Shevchenko A (2009) Global analysis of the yeast lipidome by quantitative shotgun mass spectrometry. *Proc Natl Acad Sci USA* 106: 2136–2141
- Elbaz-Alon Y, Eisenberg-Bord M, Shinder V, Stiller SB, Shimoni E, Wiedemann N, Geiger T, Schuldiner M (2015) Lam6 regulates the extent of contacts between organelles. *Cell Rep* 12: 7–14
- Emsley P, Lohkamp B, Scott WG, Cowtan K (2010) Features and development of Coot. *Acta Crystallogr D Biol Crystallogr* 66: 486–501
- Gatta AT, Wong LH, Sere YY, Calderon-Norena DM, Cockcroft S, Menon AK, Levine TP (2015) A new family of StART domain proteins at membrane contact sites has a role in ER-PM sterol transport. *Elife* 4: e07253
- Ghai R, Du X, Wang H, Dong J, Ferguson C, Brown AJ, Parton RG, Wu JW, Yang H (2017) ORP5 and ORP8 bind phosphatidylinositol-4, 5-bisphosphate (PtdIns(4,5)P₂) and regulate its level at the plasma membrane. *Nat Commun* 8: 757
- Hendrickson WA (1991) Determination of macromolecular structures from anomalous diffraction of synchrotron radiation. *Science* 254: 51–58
- Horvath MP, George EW, Tran QT, Baumgardner K, Zharov G, Lee S, Sharifzadeh H, Shihab S, Mattinson T, Li B, Bernstein PS (2016) Structure of the lutein-binding domain of human StARD3 at 1.74 Å resolution and model of a complex with lutein. *Acta Crystallogr F Struct Biol Commun* 72: 609–618
- laea DB, Dikiy I, Kiburu I, Eliezer D, Maxfield FR (2015) STARD4 membrane interactions and sterol binding. *Biochemistry* 54: 4623–4636
- Im YJ, Raychaudhuri S, Prinz WA, Hurley JH (2005) Structural mechanism for sterol sensing and transport by OSBP-related proteins. *Nature* 437: 154–158
- John K, Kubelt J, Muller P, Wustner D, Herrmann A (2002) Rapid transbilayer movement of the fluorescent sterol dehydroergosterol in lipid membranes. *Biophys J* 83: 1525–1534
- Kabsch W (1993) Automatic processing of rotation diffraction data from crystals of initially unknown symmetry and cell constants. *J Appl Crystallogr* 26: 795–800
- Kentala H, Weber-Boyvat M, Olkkonen VM (2016) OSBP-related protein family: mediators of lipid transport and signaling at membrane contact sites. *Int Rev Cell Mol Biol* 321: 299–340
- Koag MC, Cheun Y, Kou Y, Ouzon-Shubeita H, Min K, Monzingo AF, Lee S (2013) Synthesis and structure of 16,22-diketocholesterol bound to oxysterol-binding protein Osh4. *Steroids* 78: 938–944
- Kudo N, Kumagai K, Tomishige N, Yamaji T, Wakatsuki S, Nishijima M, Hanada K, Kato R (2008) Structural basis for specific lipid recognition by CERT responsible for nonvesicular trafficking of ceramide. *Proc Natl Acad Sci USA* 105: 488–493
- Lahiri S, Toulmay A, Prinz WA (2015) Membrane contact sites, gateways for lipid homeostasis. *Curr Opin Cell Biol* 33: 82–87
- Landau M, Mayrose I, Rosenberg Y, Glaser F, Martz E, Pupko T, Ben-Tal N (2005) ConSurf 2005: the projection of evolutionary conservation scores of residues on protein structures. *Nucleic Acids Res* 33: W299–W302
- Lavigne P, Najmanovich R, Lehoux JG (2010) Mammalian StAR-related lipid transfer (START) domains with specificity for cholesterol: structural conservation and mechanism of reversible binding. *Subcell Biochem* 51: 425–437
- Lees JA, Messa M, Sun EW, Wheeler H, Torta F, Wenk MR, De Camilli P, Reinisch KM (2017) Lipid transport by TMEM24 at ER-plasma membrane contacts regulates pulsatile insulin secretion. *Science* 355: eaah6171
- Letourneau D, Lefebvre A, Lavigne P, LeHoux JG (2015) The binding site specificity of STARD4 subfamily: breaking the cholesterol paradigm. *Mol Cell Endocrinol* 408: 53–61
- Maeda K, Anand K, Chiapparino A, Kumar A, Poletto M, Kaksonen M, Gavin AC (2013) Interactome map uncovers phosphatidylserine transport by oxysterol-binding proteins. *Nature* 501: 257–261
- Mathieu AP, Fleury A, Ducharme L, Lavigne P, LeHoux JG (2002) Insights into steroidogenic acute regulatory protein (StAR)-dependent cholesterol transfer in mitochondria: evidence from molecular modeling and structure-based thermodynamics supporting the existence of partially unfolded states of StAR. *J Mol Endocrinol* 29: 327–345
- Mesmin B, Pipalia NH, Lund FW, Ramlall TF, Sokolov A, Eliezer D, Maxfield FR (2011) STARD4 abundance regulates sterol transport and sensing. *Mol Biol Cell* 22: 4004–4015
- Moser von Filseck J, Copic A, Delfosse V, Vanni S, Jackson CL, Bourguet W, Drin G (2015a) INTRACELLULAR TRANSPORT. Phosphatidylserine transport by ORP/Osh proteins is driven by phosphatidylinositol 4-phosphate. *Science* 349: 432–436
- Moser von Filseck J, Vanni S, Mesmin B, Antony B, Drin G (2015b) A phosphatidylinositol-4-phosphate powered exchange mechanism to create a lipid gradient between membranes. *Nat Commun* 6: 6671
- Murcia M, Faraldo-Gomez JD, Maxfield FR, Roux B (2006) Modeling the structure of the StART domains of MLN64 and StAR proteins in complex with cholesterol. *J Lipid Res* 47: 2614–2630
- Murley A, Sarsam RD, Toulmay A, Yamada J, Prinz WA, Nunnari J (2015) Ltc1 is an ER-localized sterol transporter and a component of ER-mitochondria and ER-vacuole contacts. *J Cell Biol* 209: 539–548
- Murley A, Yamada J, Niles BJ, Toulmay A, Prinz WA, Powers T, Nunnari J (2017) Sterol transporters at membrane contact sites regulate TORC1 and TORC2 signaling. *J Cell Biol* 216: 2697–2689
- Pei J, Grishin NV (2014) PROMALS3D: multiple protein sequence alignment enhanced with evolutionary and three-dimensional structural information. *Methods Mol Biol* 1079: 263–271
- Raychaudhuri S, Im YJ, Hurley JH, Prinz WA (2006) Nonvesicular sterol movement from plasma membrane to ER requires oxysterol-binding protein-related proteins and phosphoinositides. *J Cell Biol* 173: 107–119
- Reinisch KM, De Camilli P (2016) SMP-domain proteins at membrane contact sites: structure and function. *Biochim Biophys Acta* 1861: 924–927
- Roderick SL, Chan WW, Agate DS, Olsen LR, Vetting MW, Rajashankar KR, Cohen DE (2002) Structure of human phosphatidylcholine transfer protein in complex with its ligand. *Nat Struct Biol* 9: 507–511
- Romanowski MJ, Soccio RE, Breslow JL, Burley SK (2002) Crystal structure of the *Mus musculus* cholesterol-regulated START protein 4 (StarD4) containing a StAR-related lipid transfer domain. *Proc Natl Acad Sci USA* 99: 6949–6954

- Roostae A, Barbar E, Lavigne P, LeHoux JG (2009) The mechanism of specific binding of free cholesterol by the steroidogenic acute regulatory protein: evidence for a role of the C-terminal alpha-helix in the gating of the binding site. *Biosci Rep* 29: 89–101
- Saheki Y, Bian X, Schauder CM, Sawaki Y, Surma MA, Klose C, Pincet F, Reinisch KM, De Camilli P (2016) Control of plasma membrane lipid homeostasis by the extended synaptotagmins. *Nat Cell Biol* 18: 504–515
- de Saint-Jean M, Delfosse V, Douguet D, Chicanne G, Payrastre B, Bourguet W, Antonny B, Drin G (2011) Osh4p exchanges sterols for phosphatidylinositol 4-phosphate between lipid bilayers. *J Cell Biol* 195: 965–978
- Schauder CM, Wu X, Saheki Y, Narayanaswamy P, Torta F, Wenk MR, De Camilli P, Reinisch KM (2014) Structure of a lipid-bound extended synaptotagmin indicates a role in lipid transfer. *Nature* 510: 552–555
- Steck TL, Ye J, Lange Y (2002) Probing red cell membrane cholesterol movement with cyclodextrin. *Biophys J* 83: 2118–2125
- The PyMOL Molecular Graphics System VS, LLC *The PyMOL molecular graphics system, version 1.5.0.4*. Schrödinger, LLC
- Thorsell AG, Lee WH, Persson C, Siponen MI, Nilsson M, Busam RD, Kotenyova T, Schuler H, Lehtio L (2011) Comparative structural analysis of lipid binding START domains. *PLoS ONE* 6: e19521
- Tilley SJ, Skippen A, Murray-Rust J, Swigart PM, Stewart A, Morgan CP, Cockcroft S, McDonald NQ (2004) Structure-function analysis of human [corrected] phosphatidylinositol transfer protein alpha bound to phosphatidylinositol. *Structure* 12: 317–326
- Tsujishita Y, Hurley JH (2000) Structure and lipid transport mechanism of a StAR-related domain. *Nat Struct Biol* 7: 408–414
- Vordtriede PB, Doan CN, Tremblay JM, Helmkamp GM Jr, Yoder MD (2005) Structure of PITPbeta in complex with phosphatidylcholine: comparison of structure and lipid transfer to other PITP isoforms. *Biochemistry* 44: 14760–14771
- Wong LH, Copic A, Levine TP (2017) Advances on the transfer of lipids by lipid transfer proteins. *Trends Biochem Sci* 42: 516–530
- Yeung T, Gilbert GE, Shi J, Silvius J, Kapus A, Grinstein S (2008) Membrane phosphatidylserine regulates surface charge and protein localization. *Science* 319: 210–213